

Assessment of Capture Cross Sections and Effective Density of Electron Traps Generated in Silicon Dioxides

Mo Huai Chang, Jian F. Zhang, and Wei D. Zhang

Abstract—Generation of acceptor-like electron traps in gate oxides is an important source for device instability. Despite previous efforts, capture cross sections are not unambiguously determined, and there is confusion on how many capture cross sections genuinely exist. Neither is the dependence of trap density for a given capture cross section on stress level clear. The objective of this paper is to fill this knowledge gap by investigating electron-trapping kinetics. There are a number of obstacles for such an investigation including the simultaneous occurrence of trapping and trap generation, stability of trapping, and effects of positive charges. Through careful selection of experimental conditions and testing samples, the authors have been able to overcome these obstacles. In particular, their recent work in this area has allowed them to develop a new method for correcting the effect of positive charges. After removing all uncertainties, the authors are able to identify a capture cross section as large as 10^{-13} – 10^{-14} cm² for the generated acceptorlike trap. It will be shown that electron trapping follows the first-order model, and there is also a smaller capture cross section in the region of 10^{-15} – 10^{-16} cm². To the best of their knowledge, for the first time, the authors will show that the density of the larger trap increases with stress, but the density of the smaller trap clearly saturates.

Index Terms—Defects, gate oxides, instabilities, reliability, space charges, traps.

I. INTRODUCTION

WHEN THE FIRST transistor was invented in 1947 at Bell Laboratories, it was based on Germanium. A key factor for silicon's success is the availability of silicon dioxides (SiO₂), which have excellent insulating properties and a near perfect interface with Si. The quality of SiO₂, however, will degrade during device operation, mainly because high electrical field strength in modern devices generates defects [1]–[15]. Three important types of defects have been reported: electron traps [1]–[5], interface states [1], [6], [7], and hole traps [8]–[11]. In this paper, we only address the acceptorlike electron traps.

Electron traps can be both “as-grown” or created after device fabrication. Early efforts were focused on the as-grown traps [12]–[14]. It was found that as-grown traps originated from impurities in the oxide, such as water molecules [12] and

implants [13]. For a modern MOSFET, however, the use of poly-Si gates and a careful control of impurities have effectively eliminated these as-grown traps [15]. As a result, we will focus on the generated electron traps here.

Generated electron traps play an important role in device reliability. They can have several adverse effects on the device performance, such as a shift in device parameters [1], [5] and stress-induced leakage current (SILC) [16]–[18]. As their number accumulates, they can form a conduction path between gate and substrate, which leads to oxide breakdown [4], [17]–[19]. For a high- κ /SiO₂ stack, it has been suggested that its breakdown can be controlled by the interfacial SiO₂ layer [20]. Consequently, generated traps are important for the stack as well. Despite of past efforts, there are unsolved issues. For example, capture cross sections are not unambiguously determined and there are confusions on how many capture cross sections genuinely existing. The dependence of a trap density for a given capture cross section on stress level is not clear, either. There is a lack of techniques for correcting the positive-charge effect on electron trapping. The objective of this paper is to fill this knowledge gap by investigating electron-trapping kinetics.

The most well known trapping model is the first-order model [12]–[14]. It was applied successfully for as-grown electron traps [12], [13]. Although it was proposed that this model could also be applied for generated traps [5], this verdict has not been adopted generally. Most of the previous works on generated electron traps did not address the trapping kinetics because of a number of obstacles, as summarized below.

First, for thin oxides (< 3 nm), traps can be located sufficiently close to the electrodes that trapped electrons can tunnel away. In this case, trapping will not be stable, and it is difficult to study the kinetics. The SILC has been widely used as a measure of generated defects in thin oxides [18]. However, electron traps are not the only source for SILC [16]. The important trapping parameters, such as capture cross sections and density, were rarely reported from the work based on SILC.

Second, if relatively thick oxide is used, stable electron trapping can be achieved, but the difficulty is in separating the trap filling from the trap creation. In most of the previous works, electrons were injected into the oxide during trap generation. Once the traps are generated, these electrons can fill the traps. Since the filling is typically much faster than the creation, the trapping level is determined by the generation rather than

Manuscript received June 13, 2005; revised October 28, 2005. The work of M. H. Chang and W. D. Zhang was supported by the Liverpool John Moores University during their Ph.D. study. The review of this paper was arranged by Editor T. Skotnicki.

The authors are with the School of Engineering, Liverpool John Moores University, Liverpool L3 3AF, U.K. (e-mail: J.F.Zhang@livjm.ac.uk).

Digital Object Identifier 10.1109/TED.2006.874155

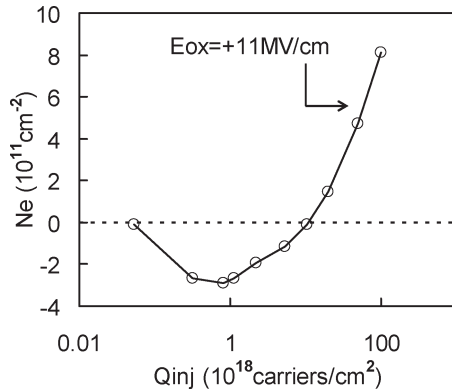


Fig. 1. Electron-trapping density N_e during stresses under an oxide field of $+11$ MV/cm. N_e is negative initially due to the positive-charge formation. As the electron traps are generated and filled, N_e becomes positive, which represents net negative charges. The trap generation and filling processes cannot be separated here, and the data cannot be used for studying the kinetics of trap filling.

filling. One example is given in Fig. 1. Here, one MOSFET was subjected to Fowler–Nordheim injection (FNI). The electron trapping density N_e is negative initially, indicating net positive charges. As the stress increases, N_e becomes positive, which represents net negative charges, and builds up continuously without saturation. The nonsaturation of N_e observed here results from the continuous creation of new traps rather than filling the existing traps. As a result, it cannot be used for studying the kinetics of trap filling.

Third, recent works [8]–[11] show that electrical stresses generate not only electron traps but also hole traps. Hole trapping leads to positive-charge formation in the oxide, which offsets electron trapping. This complicates the study, and care must be exercised to take it into account.

To investigate the trapping kinetics of generated electron traps, the obstacles mentioned above must be overcome. We believe that this can be achieved now, since recent works have improved our understanding of both electron traps [15], [21] and hole traps [8]–[11]. Through careful selection of test conditions and samples, unambiguous results have been obtained on trap capture cross sections and densities.

II. DEVICES AND EXPERIMENTS

A. Devices

When selecting testing samples and stress techniques, priority is given to overcome the obstacles mentioned earlier and to simplify the test conditions as far as possible. To avoid the uncertainty caused by the use of SILC for measuring electron traps, we chose relatively thick oxide (7 nm) here, since it gives stable electron trapping in large quantities ($\sim 10^{12}$ cm $^{-2}$). In agreement with the early works [4], [22], we found that electron-trap properties were insensitive to oxide thickness (Section IV-D). The selected stress technique requires the use of pMOSFETs as testing samples. They have a surface channel and p+ poly-Si gate. The n -well was heavily doped, and no threshold-voltage adjustment implantation was carried out. The channel length is 10 μ m, and the channel width is 200 μ m. Each device has five terminals. Apart from gate, source, and

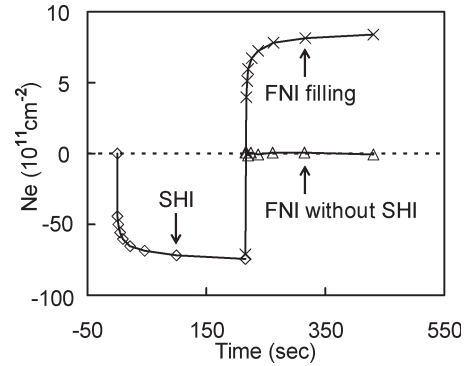


Fig. 2. Typical test procedures. A device was stressed by SHI (SHI, oxide field: $E_{ox} = -5$ MV/cm, n -well bias: 8.8 V; p-substrate bias: 9.8 V) during which positive charges were formed through hole trapping. After SHI, electrons were injected into the oxide under $E_{ox} = +8$ MV/cm for filling the generated electron traps and neutralizing the positive charges (symbol “x”). If $E_{ox} = +8$ MV/cm is applied to a fresh device (symbol “ Δ ”), there is little trapping, which indicates that the trap generation by the filling step itself is negligible.

drain, it has contacts to n -well and p-substrate, which allows the substrate hole injection (SHI) and charge pumping to be carried out [6]–[10].

B. Experiments

To remove the uncertainty in the lateral distribution of the generated traps, we will stress the devices uniformly. Uniform stress has been used in many early works (e.g., [16], [18], [23]) and it can be achieved by either FNI [5] or substrate hole/electron injection [18], [23], [24]. Since electrons are injected into the oxide under both FNI and substrate electron injection, generated traps can be filled during the stress. Consequently, the generation phase is not clearly separated from the filling process, which complicates the investigation of trapping kinetics. During the SHI, electron injection was negligible, and positive charges were built up through hole trapping, as is shown in Fig. 2. Generated electron traps are neutral during the stress, since there were no electrons available for filling them. A subsequent electron injection was applied to fill these traps. As a result, the trap-filling process is separated from the generation phase, allowing the investigation of trapping kinetics. We chose SHI for creating electron traps in this paper.

Unless otherwise specified, SHI will be carried out under an oxide field of $E_{ox} = -5$ MV/cm, an n -well bias of 8.8 V, and a p-substrate bias of 9.8 V. The trap filling is carried out under $E_{ox} = +8$ MV/cm with all other terminals grounded. Additional trap generation by the filling step itself was found being negligible, as shown in Fig. 2. The trapped charge density was measured from the gate-voltage shift at the midgap of the n -well, where the contribution from the generated interface states is negligible [25]. The measurement takes a few seconds, and there is no doubt that the electrons trapped very close to the electrodes will escape. These traps will not be studied in this paper. Since the charge centroid is not known, we follow the well-accepted practice and use the “effective trap density” N_e by assuming the centroid to be at the oxide/substrate interface [15], [21]. Further details of experiments can be found from our earlier works [15], [21], [24].

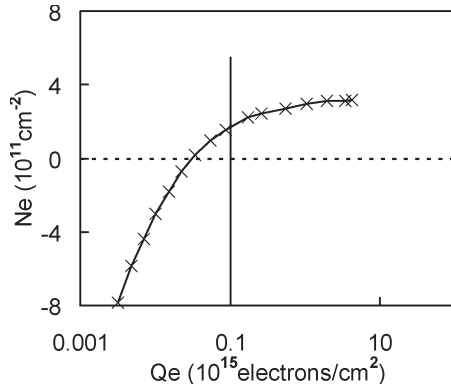


Fig. 3. Device was stressed by SHI with a hole fluency of 10^{15} cm^{-2} . At low level of electron injection Q_e during the filling, N_e was initially negative, which represents net positive charges. This is because neutralization of as-grown hole traps was not completed until Q_e reached 10^{14} cm^{-2} , approximately. As a result, the data for $Q_e < 10^{14} \text{ cm}^{-2}$ will not be used for studying the trapping kinetics in this paper. To facilitate the measurement at low Q_e , $E_{ox} = +6.5 \text{ MV/cm}$ is used here.

III. EFFECTS OF POSITIVE CHARGES

A. Low Stress Level

After obtaining stable electron trapping and separating the trap filling from the generation, a remaining obstacle for studying the electron-trapping kinetics is the offsetting effects of positive charges. When hole fluency during the SHI stress N_h is relatively low (e.g., $N_h < 10^{16} \text{ hole/cm}^2$), hole trapping is dominated by as-grown hole traps. These are hole traps preexisted in the device after fabrication. After stopping the hole injection and starting the electron injection, electron traps are filled and positive charges are neutralized, as shown in Figs. 2 and 3. When the electron fluency for filling Q_e is below 10^{14} cm^{-2} approximately, Fig. 3 shows that as-grown hole traps are not fully neutralized and the measured N_e is the “net” charge. This means that electron-trapping kinetics for acceptorlike traps cannot be investigated in the region of $Q_e < 10^{14} \text{ cm}^{-2}$.

Earlier works [9], [21], [26] showed that the neutralization of as-grown hole traps was completed when electron fluency reached the level of 10^{14} cm^{-2} . Consequently, the electron trapping for $Q_e > 10^{14} \text{ cm}^{-2}$ is not affected by the as-grown hole trapping. As a result, only N_e measured at $Q_e > 10^{14} \text{ cm}^{-2}$ will be used for studying the electron-trapping kinetics in this paper. The impact of a lack of data for $Q_e < 10^{14} \text{ cm}^{-2}$ will be discussed in Section IV-B.

B. High Stress Level

Typical test results are given in Fig. 4. As the stress level increases, more traps were generated and the whole trapping curve moves up, when the hole fluency N_h is less than $10^{16} \text{ hole/cm}^2$. When N_h rises further, however, the increase of trapping disappears at relatively low Q_e , although trapping is still clearly increased at higher Q_e . This is because considerable amount of new hole traps was created at higher N_h [8]–[11]. Although as-grown hole traps have an energy level below the bottom edge of the silicon-conduction band, some of the generated hole traps have energy levels above it, as illustrated

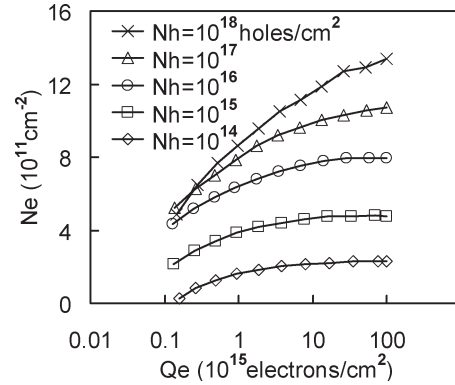


Fig. 4. Electron trapping after different levels of stresses by SHI. When the hole fluency N_h is less than 10^{16} cm^{-2} , an increase in N_h leads to a higher N_e over the whole range of Q_e . For $N_h > 10^{16} \text{ cm}^{-2}$, however, N_e increases at high Q_e , but this increase is suppressed at low Q_e .

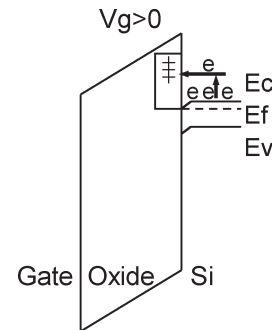


Fig. 5. Energy band diagram for ANPCs. ANPC has energy levels above the bottom edge of silicon-conduction band. The higher the energy level, the less electrons are available in silicon and the more difficult for neutralizing a positive charge.

in Fig. 5 [9]–[11]. Since the number of electrons in the silicon-conduction band drops rapidly for higher energy level, the number of electrons available for neutralizing these generated hole traps is less than that for as-grown hole traps. As a result, it is more difficult to neutralize these generated hole traps, and they are called “antineutralization positive charges (ANPC)” [9]–[11]. When the Q_e in Fig. 4 is relatively low, the neutralization of ANPC is not completed, and the remaining positive ANPC brings down N_e through offsetting. As Q_e increases further, ANPC is gradually neutralized, which leads to higher N_e for higher N_h . Since the ANPC has a substantial effect on the dynamic behavior of N_e , it is essential to correct this effect before the trapping kinetics of generated electron traps can be investigated. A correction method is proposed below.

In Fig. 6(a), a device was heavily stressed by SHI, which created ANPC. After the stress, the electrons were injected into the oxide to fill the generated electron traps and neutralize the positive charges, and symbol “ Δ ” represents the net charge density. This is followed by applying a negative gate bias (symbol “o”), during which both filled electron traps and neutralized ANPC can lose their electrons through electron tunneling to silicon, resulting in the drop of N_e . Electron injection was then switched on again in an attempt to refill them (symbol “x”). In Fig. 6(b), the trapping density during the first and second filling is compared. It is obvious that the trapping during the second filling failed to reach the same level as that for the

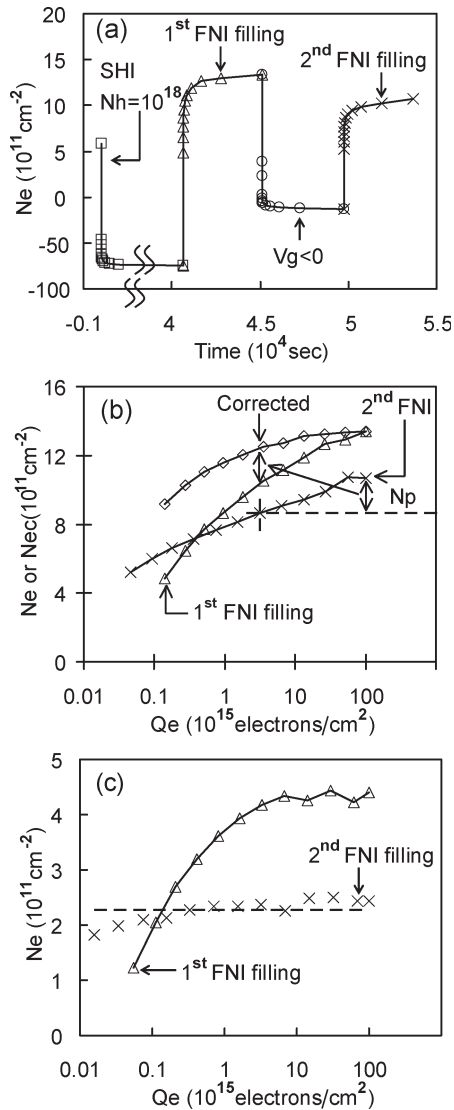


Fig. 6. Method for correcting the offset effect of ANPCs on Ne. (a) Device was heavily stressed by SHI with $N_h = 10^{18}$ hole/cm², which generated not only electron traps but also ANPC. During the following “first FNI filling,” the electron traps captured electrons and became negative, and the positive charges were neutralized. This led to the rise of the net electron trapping (symbol “ Δ ”). A negative gate bias ($V_g < 0$, $E_{ox} = -5$ MV/cm) was then applied. Under $V_g < 0$, both filled electron traps and neutralized ANPC can lose their electrons through tunneling, which resulted in the fall of Ne (symbol “ \circ ”). When the electron injection was resumed (the “second FNI filling”), the detrapped electron traps cannot recapture electrons, and the rise represented by symbol “ \times ” is entirely from the reneutralizing ANPC. (b) Data represented by the symbols “ Δ ” and “ \times ” in (a) are replotted against Q_e . At a given level of Q_e , the remaining positive ANPC is represented by N_p . The correct electron trapping level is the net trapping (symbol “ Δ ”) plus N_p and is shown as the symbol “ \diamond .” (c) Test procedure shown in (a) was used again, but N_h was limited at 10^{15} hole/cm², which is sufficiently low that creation of ANPC is not significant. (c) shows that the lack of ANPC leads to a nearly flat Ne during the second filling. The dashed line is a guide for the eye.

first filling. Our recent work [21] shows that this is because the electron trap cannot recapture an electron, after detrapping through tunneling, although the ANPC can [9]–[11]. To further illustrate the difference of generated electron traps and ANPC in refilling, the test procedure in Fig. 6(a) was used again, but the hole fluency was chosen to be sufficiently low this time that the creation of ANPC is insignificant. With little ANPC, Fig. 6(c) shows that the rise of Ne during the second filling

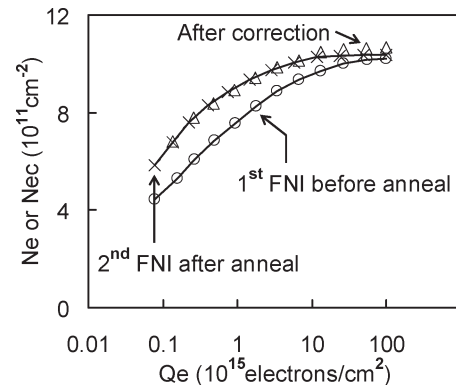


Fig. 7. Two devices were subjected to the same stress of $N_h = 10^{17}$ cm⁻². After filling the traps (symbol “ \circ ”), one of them was annealed at 150 °C for 160 min to remove the ANPC. After annealing the ANPC, a short SHI ($N_h = 10^{15}$ cm⁻²) was used to empty all the electron traps before they were refilled (the symbol “ \times ”). The other device went through the test sequence shown in Fig. 6(a), and the effect of positive charges was corrected by following the method shown in Fig. 6(b). The corrected data are represented by symbol “ Δ .” The good agreement between the trapping after annealing ANPC and that after the correction supports the correction method strongly.

is also insignificant. The nearly flat Ne (see the dashed line) confirms that, after tunneling-induced detrapping, an electron trap cannot capture an electron again. Consequently, the rise of Ne during the second filling in Fig. 6(b) can only originate from the reneutralization of ANPC.

We are now in a position to correct the offsetting effect of positive charges on electron trapping. The real level of electron trapping Nec can be found from

$$Nec = Ne + Np \quad (1)$$

where Ne is the net trapping and is directly measured. The key question is how to estimate N_p . As explained earlier, the rise of Ne during the second filling in Fig. 6(b) originates from the reneutralization of the positive charges. As a result, the amount of positive charges neutralized between a given Q_e and the end of filling is

$$N_p(Q_e) = Ne(\text{End of second filling}) - Ne(Q_e \text{ of second filling}). \quad (2)$$

In other words, the unneutralized positive charge at Q_e is N_p , as shown in Fig. 6(b). Once N_p is known, the real level of trapping can be found from (1) and is plotted in Fig. 6(b).

C. Support for the Correction Method

Our recent work shows that the ANPC is thermally unstable and can be annealed at 150 °C [9]. In Fig. 7, two devices were subjected to the same stresses with $N_h = 10^{17}$ cm⁻². After filling the generated electron traps, one device was exposed to 150 °C for 160 min to remove the ANPC. A short hole injection ($N_h = 10^{15}$ cm⁻²) was then used to empty the electron traps still filled at the end of the thermal exposure. This short hole injection is too low to recreate the ANPC [9], [11]. When the traps were refilled (symbol “ \times ”), Ne was obviously enhanced at low Q_e but remain essentially the same at the end of the filling. This supports our assumption that positive ANPC lowers the

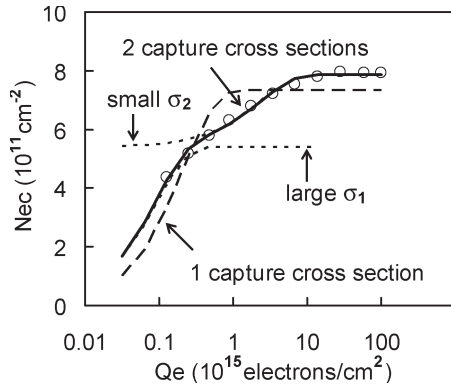


Fig. 8. Trapping kinetics of electron traps generated by SHI with $N_h = 10^{16} \text{ cm}^{-2}$. The dashed and solid lines were obtained by fitting the data with (3) and (4), respectively. The two dotted lines show the contribution of traps with large ($\sigma_1 = 1.1 \times 10^{-14} \text{ cm}^2$) and small ($\sigma_2 = 4.2 \times 10^{-16} \text{ cm}^2$) capture cross sections.

measured Ne at low Qe. As Qe increases, ANPC is neutralized and Ne approaches the true level of electron trapping. The other devices went through the test sequence shown in Fig. 6(a), and the effect of positive charges was corrected by the proposed method. Fig. 7 compares the corrected trapping density (symbol “ Δ ”) with the measured Ne after annealing. The trapping after correction for positive charges agrees well with the trapping after ANPC is thermally annealed. This strongly supports the newly proposed correction method.

IV. TRAPPING KINETICS AND TRAP PROPERTIES

A. First-Order Model

After correcting the effect of positive charges on the electron trapping, we are ready to study the trapping kinetics of the generated electron traps and assess the trap properties. The simplest model is the first-order model with a single capture cross section σ . It can be expressed as [5]

$$N_e = N_s [1 - \exp(-\sigma Q_e)]. \quad (3)$$

As the electron fluency Qe increases, this model predicts that trapping will saturate at a level of N_s . Such saturation is indeed observed in Fig. 8. However, the correlation between the experimental data and (3) (dashed line) is poor. The correlation can be improved (solid line) by assuming that there are two capture cross sections for generated traps, namely

$$N_e = N_{s1} [1 - \exp(-\sigma_1 Q_e)] + N_{s2} [1 - \exp(-\sigma_2 Q_e)]. \quad (4)$$

The extracted capture cross sections are $\sigma_1 = 1.1 \times 10^{-14} \text{ cm}^2$ and $\sigma_2 = 4.2 \times 10^{-16} \text{ cm}^2$. Here, the adjustable parameters have been increased from two (N_s and σ) in (3) to four (N_{s1} , σ_1 , N_{s2} , and σ_2) in (4). As a result, the improved correlation may simply result from this increase in adjustable parameters. Indeed, one may say that an excellent agreement between the experimental data and a model can always be achieved if the model contains enough adjustable parameters. In fact, this is where many researchers have their reservations about the validation of the first-order model. The use of two capture cross sections in (4) must be further supported.

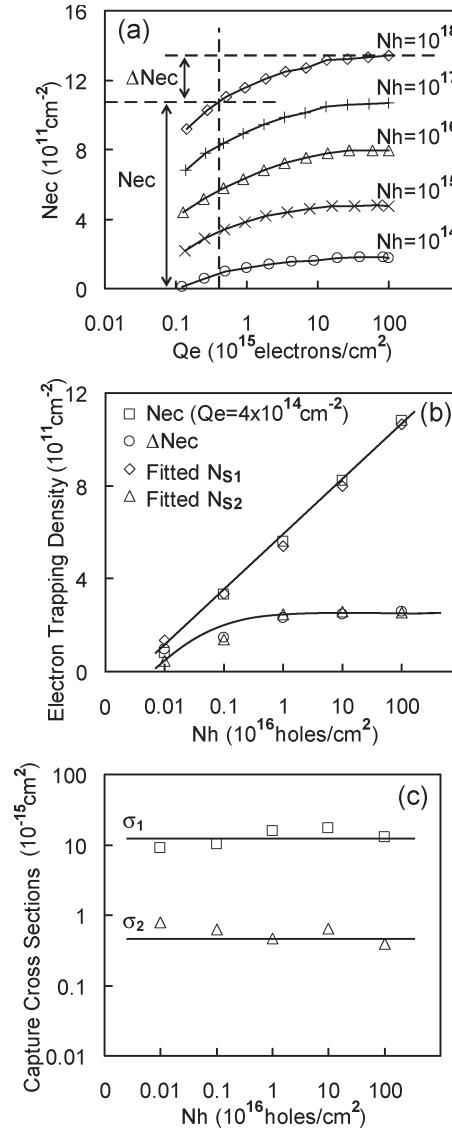


Fig. 9. Supports for the presence of two capture cross sections. (a) Shows the corrected trapping Nec after different levels of stresses. The unit of Nh in the figure is holes/cm². The Nec at $Q_e = 4 \times 10^{14} \text{ cm}^{-2}$, and the subsequent trapping ΔN_{ec} is marked out for $N_h = 10^{18} \text{ holes/cm}^2$. (b) Shows the extracted N_{s1} and N_{s2} together with Nec ($Q_e = 4 \times 10^{14} \text{ cm}^{-2}$) and ΔN_{ec} . The different dependences of N_{s1} and N_{s2} on stresses indicate that they originate from two different defects. This supports the presence of two capture cross sections strongly. (c) Shows that the extracted two capture cross sections are insensitive to stress levels.

B. Support for the Presence of Two Capture Cross Sections

After correcting the offset effect by positive charges, electron-trapping-post different stress levels are plotted in Fig. 9(a). When compared with the data before correction in Fig. 4, the trapping is higher over the whole range of Qe now for larger Nh, because a larger Nh generated more traps. Supports for the existence of two genuine capture cross sections can be obtained by examining their dependence on stress levels, as detailed below.

1) *Different Dependence of Trap Densities on Stress Levels:* On one hand, if the two capture cross sections originated from the same defect, the improved correlation would be an artifact, since there were no evidences for the same defect possessing

two well separated capture cross sections. On the other hand, if we can show that these two capture cross sections originate from two different defects, it will support the existence of two capture cross sections strongly.

When there are two different electron traps, it is possible that their densities can change independently as the stresses increase. Fig. 9(b) shows that this is the case. As the stresses increase, the effective density of the larger trap ($\sigma_1 : 10^{-13} \sim 10^{-14} \text{ cm}^2$) N_{s1} increases continuously. In contrast, the effective density of the smaller trap ($\sigma_2 : 10^{-15} \sim 10^{-16} \text{ cm}^2$), N_{s2} , clearly saturates. If they were from the same defect, they should increase simultaneously, which is against Fig. 9(b). Consequently, our results strongly support the presence of two different electron traps with well-separated capture cross sections.

2) *Insensitivity of Extracted Capture Cross Sections to Stress Levels:* If there exist two capture cross sections, the same values should be observed at all stress levels. Fig. 9(c) shows that the two extracted capture cross sections are indeed insensitive to stress levels, further supporting our claim.

3) *Agreement With Direct Observations:* Fig. 9(a) shows that, after correcting the effects of the positive charges, the curves are nearly a parallel upward shift as the stresses increase. This indicates that the increase in trapping mainly occurs at low Q_e , while the increase is insignificant for further trapping as Q_e becomes higher. To show this more clearly and to avoid curve fitting, we plotted the N_{ec} at $Q_e = 4 \times 10^{14} \text{ cm}^{-2}$ and $\Delta N_{ec} = N_{ec}(Q_e = 10^{17} \text{ cm}^{-2}) - N_{ec}(4 \times 10^{14} \text{ cm}^{-2})$ in Fig. 9(b). The former rises continuously and the latter clearly saturates, indicating the presence of two different trapping processes. This behavior agrees well with that of the extracted trap densities.

Finally, we would like to point out that the lack of data for $Q_e < 10^{14} \text{ cm}^{-2}$ will affect the accuracy of the extracted larger capture cross (σ_1). This is because its filling partially occurs in the region of $Q_e < 10^{14} \text{ cm}^{-2}$, where no reliable data are available. However, Fig. 9(a) shows that electron trapping at $Q_e = 10^{14} \text{ cm}^{-2}$ is substantial, and there is no doubt that some acceptorlike traps have an effective physical size in the order of $10^{-13} - 10^{-14} \text{ cm}^2$. The order of magnitude of σ_1 will not be changed by the lack of data for $Q_e < 10^{14} \text{ cm}^{-2}$. The identification of such a large capture cross section for an acceptorlike electron trap is an achievement of this paper, since it can be often masked by the offsetting effect of positive charges. Its large effective physical size and nonsaturating nature indicate that it will play an important role in the oxide breakdown and SILC, which need further investigation.

C. Comparison of Electron Traps Created With and Without Electron Injection During Stresses

Up to the present, we have only studied electron traps created by SHI. In most of previous works, electrons were injected into the oxide during stresses. The question is whether the same traps were created in these two cases or not and they are compared next.

Fig. 10(a) shows the test procedure. A device was first stressed by Fowler-Nordheim (FN) electron injection. As mentioned earlier, the electrons injected during the stress can fill the generated traps. To study the trapping kinetics, the filled

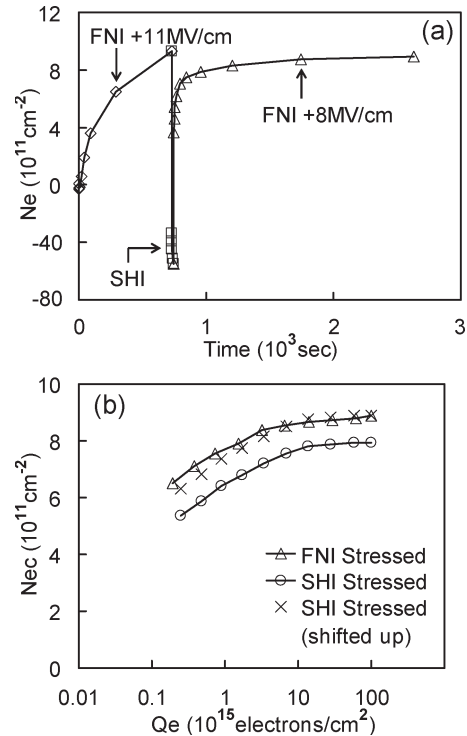


Fig. 10. Comparison of electron traps created by FNI and SHI. (a) Shows the test procedure. A device was stressed by FN injection at $E_{ox} = +11 \text{ MV/cm}$ until an electron fluency of 10^{20} cm^{-2} was reached. To study the trapping kinetics, the traps filled during the stress were emptied by a short SHI with $N_h = 10^{15} \text{ hole/cm}^2$ and then refilled under $E_{ox} = +8 \text{ MV/cm}$ (symbol “ Δ ”). (b) Compares the dynamic-filling behavior of the traps created by FNI with that by SHI ($N_h = 10^{16} \text{ hole/cm}^2$). The N_e after FNI was corrected by the method given in Fig. 6(a) and (b). To clearly show that the trapping kinetics is similar in these two cases, the trapping after SHI was shifted upward to give the symbol “ \times .”

electron traps were first emptied by using a short hole injection and then refilled. The trapping kinetics of the traps generated by FNI is compared with that by SHI in Fig. 10(b). The trapping kinetics is obviously similar in these two cases, indicating that the same traps were created.

D. Impact of Oxide Thickness on the Generated Traps

Up to the present, only a 7-nm oxide is used in this paper. It is of interest to find out if the extracted capture cross sections are sensitive to oxide thickness. Fig. 11 compares the trapping kinetics for a 13.8- and a 7-nm oxide. It is clear that the extracted capture cross sections are essentially the same for samples of different thickness. This is in agreement with the early works, which showed that the properties of generated electron traps were insensitive to oxide thickness [4], [22].

V. CONCLUSION

To improve our understanding of the generated electron traps, trapping kinetics is investigated in this paper. By stressing the oxide with SHI, the generation phase is separated from the trap-filling phase. The use of uniform stress and filling removes the uncertainty in lateral distribution. The selection of relatively thick SiO_2 layer allows the direct measurement of trapped electron density, and the uncertainty caused by the

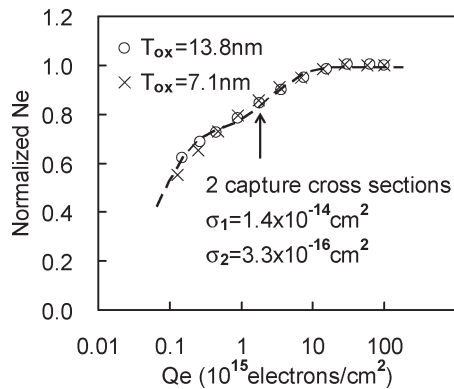


Fig. 11. Comparison of electron traps generated in oxides of different thicknesses. N_e was normalized against its saturation value. The dashed line was obtained by fitting the data with (4). It is apparent that the same two capture cross sections are present in these two samples.

use of SILC is avoided. An achievement of this paper is the development of a new method, which successfully corrected the effect of ANPCs.

After the correction, we are able to clearly observe an electron capture cross section as large as 10^{-13} – 10^{-14} cm^2 for the generated acceptorlike electron traps. The filling kinetics follows the first-order model, and there are two genuine and well separated capture cross sections. The smaller capture cross section is in the region of 10^{-15} – 10^{-16} cm^2 . To the best of our knowledge, for the first time, it is clearly shown that the density of the smaller trap saturates, while the density of the larger trap does not.

ACKNOWLEDGMENT

The authors would like to thank G. Groeseneken and R. Degraeve at Inter-university Microelectronics Center (IMEC), and C. Z. Zhao and M. Zahid at Liverpool John Moores University for the kind support. The test sample used in this work was provided by IMEC.

REFERENCES

- [1] R. Woltjer, A. Hamada, and E. Takeda, "Time dependence of p-MOSFET hot-carrier degradation measured and interpreted consistently over ten orders of magnitude," *IEEE Trans. Electron Devices*, vol. 40, no. 2, pp. 392–401, Feb. 1993.
- [2] W. Chen, A. Balasinski, and T. P. Ma, "Lateral profiling of oxide charge and interface traps near MOSFET junctions," *IEEE Trans. Electron Devices*, vol. 40, no. 1, pp. 187–196, Jan. 1993.
- [3] M. Brox and W. Weber, "Dynamic degradation in MOSFET's—Part I: The physical effects," *IEEE Trans. Electron Devices*, vol. 38, no. 8, pp. 1852–1858, Aug. 1991.
- [4] R. Degraeve, G. Groeseneken, R. Bellens, J. L. Ogier, M. Depas, P. J. Roussel, and H. E. Maes, "New insights in the relation between electron trap generation and the statistical properties of oxide breakdown," *IEEE Trans. Electron Devices*, vol. 45, no. 4, pp. 904–911, Apr. 1998.
- [5] J. F. Zhang, S. Taylor, and W. Eccleston, "Electron trap generation in thermally grown SiO_2 under Fowler–Nordheim stress," *J. Appl. Phys.*, vol. 71, no. 2, pp. 725–734, Jan. 1992.
- [6] J. F. Zhang, C. Z. Zhao, G. Groeseneken, and R. Degraeve, "An analysis of the kinetics for interface state generation following hole injection," *J. Appl. Phys.*, vol. 93, no. 10, pp. 6107–6116, May 2003.
- [7] J. F. Zhang, H. K. Sii, R. Degraeve, and G. Groeseneken, "Mechanism for the generation of interface state precursors," *J. Appl. Phys.*, vol. 87, no. 6, pp. 2967–2977, Mar. 2000.

- [8] J. F. Zhang, H. K. Sii, G. Groeseneken, and R. Degraeve, "Hole trapping and trap generation in the gate silicon dioxide," *IEEE Trans. Electron Devices*, vol. 48, no. 6, pp. 1127–1135, Jun. 2001.
- [9] J. F. Zhang, C. Z. Zhao, A. H. Chen, G. Groeseneken, and R. Degraeve, "Hole traps in silicon dioxides—Part I: Properties," *IEEE Trans. Electron Devices*, vol. 51, no. 8, pp. 1267–1273, Aug. 2004.
- [10] C. Z. Zhao, J. F. Zhang, G. Groeseneken, and R. Degraeve, "Hole traps in silicon dioxides—Part II: Generation mechanism," *IEEE Trans. Electron Devices*, vol. 51, no. 8, pp. 1274–1280, Aug. 2004.
- [11] C. Z. Zhao and J. F. Zhang, "Effects of hydrogen on positive charges in gate oxides," *J. Appl. Phys.*, vol. 97, no. 7, pp. 073703-1–073703-8, Apr. 2005.
- [12] E. H. Nicollian, C. N. Berglund, P. F. Schmidt, and J. M. Andrews, "Electrochemical charging of thermal SiO_2 films by injected electron currents," *J. Appl. Phys.*, vol. 42, no. 13, pp. 5654–5664, Dec. 1971.
- [13] R. F. DeKeersmaecker and D. J. DiMaria, "Electron trapping and detrapping characteristics of arsenic-implanted SiO_2 layers," *J. Appl. Phys.*, vol. 51, no. 2, pp. 1085–1101, Feb. 1980.
- [14] J. F. Zhang, S. Taylor, and W. Eccleston, "A quantitative investigation of electron detrapping in SiO_2 under Fowler–Nordheim stress," *J. Appl. Phys.*, vol. 71, no. 12, pp. 5989–5996, Jun. 1992.
- [15] W. D. Zhang, J. F. Zhang, M. Lalor, D. Burton, G. Groeseneken, and R. Degraeve, "Two types of neutral electron traps generated in the gate silicon dioxide," *IEEE Trans. Electron Devices*, vol. 49, no. 11, pp. 1868–1875, Nov. 2002.
- [16] D. Ielmini, A. S. Spinelli, M. A. Rigamonti, and A. L. Lacaita, "Modeling of SILC based on electron and hole tunneling—Part I: Transient effects," *IEEE Trans. Electron Devices*, vol. 47, no. 6, pp. 1258–1265, Jun. 2000.
- [17] S. Bruyere, D. Roy, E. Robilliart, E. Vincent, and G. Ghibaudo, "Body effect induced wear-out acceleration in ultra-thin oxides," *Microelectron. Reliab.*, vol. 41, no. 7, pp. 1031–1034, Jul. 2001.
- [18] D. J. DiMaria and J. H. Stathis, "Anode hole injection, defect generation, and breakdown in ultrathin silicon dioxide films," *J. Appl. Phys.*, vol. 89, no. 9, pp. 5015–5024, May 2001.
- [19] J. Sune and E. Y. Wu, "Statistics of successive breakdown events in gate oxides," *IEEE Electron Device Lett.*, vol. 24, no. 4, pp. 272–274, Apr. 2003.
- [20] R. Degraeve, T. Kauerauf, A. Kerber, E. Cartier, B. Govoreanu, P. Roussel, L. Pantisano, P. Blomme, B. Kaczer, and G. Groeseneken, "Stress polarity dependence of degradation and breakdown of SiO_2 /high- κ stacks," in *Proc. IEEE 41st Int. Reliab. Phys. Symp.*, Dallas, TX, 2003, pp. 23–28.
- [21] W. D. Zhang, J. F. Zhang, M. J. Lalor, D. R. Burton, G. Groeseneken, and R. Degraeve, "Effects of detrapping on electron traps generated in gate oxides," *Semicond. Sci. Technol.*, vol. 18, no. 2, pp. 174–182, Feb. 2003.
- [22] J. H. Stathis and D. J. DiMaria, "Oxide scaling limit for future logic and memory technology," *Microelectron. Eng.*, vol. 48, no. 1–4, pp. 395–401, Sep. 1999.
- [23] D. J. DiMaria, "Defect generation under substrate-hot-electron injection into ultrathin silicon dioxide layers," *J. Appl. Phys.*, vol. 86, no. 4, pp. 2100–2109, Aug. 1999.
- [24] M. H. Chang and J. F. Zhang, "On the role of hydrogen in hole-induced electron trap creation," *Semicond. Sci. Technol.*, vol. 19, no. 11, pp. 1333–1338, Nov. 2004.
- [25] C. E. Blat, E. H. Nicollian, and E. H. Poindexter, "Mechanism of negative-bias-temperature instability," *J. Appl. Phys.*, vol. 69, no. 3, pp. 1712–1720, Feb. 1991.
- [26] A. R. Stives and C. T. Sah, "A study of oxide traps and interface states of the silicon–silicon dioxide interface," *J. Appl. Phys.*, vol. 51, no. 12, pp. 6296–6304, Dec. 1980.



MOS devices.

Mo Huai Chang was born in Taipei, Taiwan, R.O.C., in 1978. He received the DUT degree in electrical and computer engineering from the Paris XI Cachan Institute of Technology, Paris, France, in 1999 and the B.Eng. degree in computer engineering from the Liverpool John Moores University, Liverpool, U.K., in 2000, where he is currently working toward the Ph.D. degree in electrical and electronic engineering.

His current research interests include defect generation in MOS dielectrics and the reliability of



Jian F. Zhang received the B.Eng. degree in electrical engineering from Xi'an Jiao Tong University, Xi'an, China, in 1982 and the Ph.D. degree in electrical engineering from Liverpool University, Liverpool, U.K., in 1987.

From 1986 to 1992, he was a Senior Research Assistant at the University of Liverpool, where he worked on the dielectric recovery of plasma in accelerating gas flow, plasma processing of semiconductors, and the reliability of MOS devices. In 1992, he joined the Liverpool John Moores University as a Senior Lecturer. He became a Reader in microelectronics in 1996 and a Professor in 2001. His current research interests include performance, degradation, and defect characterization of MOS devices and high- κ layers.

Dr. Zhang is a member of the technical program committee for the IEEE Semiconductor Interface Specialists Conference (SISC).

Wei D. Zhang received the B.Sc. degree in semiconductor physics and devices from the Beijing Institute of Technology, Beijing, China, in 1989, the M.Sc. degree in semiconductor devices and microelectronics from the Xidian University, Shaanxi, China, in 1992, and the Ph.D. degree in microelectronics from the Liverpool John Moores University, Liverpool, U.K., in 2003.

From 1992 to 1999, he was a Lecturer and then an Associate Professor at the Xidian University. He became a Lecturer at the Bournemouth University in 2002, and joined Liverpool John Moores University as a Senior Lecturer in 2005. His research interests cover the area of reliability of MOS devices, and the degradation and breakdown of oxide dielectrics.